Kinetics and Catalysis, Vol. 45, No. 3, 2004, pp. 436–445. Translated from Kinetika i Kataliz, Vol. 45, No. 3, 2004, pp. 463–472.

CATALYTIC REACTION MECHANISMS

Reaction Kinetics and Mechanism of Selective NO Reduction on a CoZSM-5 Catalyst as Studied by SSITKA

E. M. Sadovskaya*, A. P. Suknev*, V. B. Goncharov*, B. S. Bal'zhinimaev*, and C. Mirodatos**

** Boreskov Institute of Catalysis, Siberian Division, Russian Academy of Sciences, Novosibirsk, 630090 Russia*

*** Institut de Recherches sur la Catalyse, F 69626 Villeurbanne Cedex, France*

Received February 6, 2003

Abstract—The dynamics of ^{13}C transfer from methane to carbon dioxide was studied under the steady-state reaction conditions of selective NO reduction with methane on a CoZSM-5 catalyst at various reactant (NO, CH_4, and O_2) concentrations and temperatures. It was found that the reaction occurs by a two-pathway mechanism with the participation of Co^{2+} sites (or CoO_x clusters) and paired Co^{2+}–OH sites localized at the boundary between the clusters and the zeolite; in this case, the rate of the reaction at boundary sites was higher by more than one order of magnitude. Based on the numerical simulation of isotopic response curves, the concentrations of intermediate compounds and the rate constants of particular steps were evaluated; differences in the kinetics via the above reaction pathways were found and analyzed.

INTRODUCTION

The selective reduction of NO with methane on a CoZSM-5 catalyst is a potential process for the removal of nitrogen oxides from waste gases. It is well known that the rate of the reaction dramatically increases in the presence of oxygen [1–4] because of the formation of adsorbed [NO_x] species, which are key intermediates in the reduction of nitrogen oxides [2–6], on the catalyst surface. A great number of publications have been devoted to the nature and reactivity of [NO_x] toward hydrocarbons [4, 7–17]. According to IR-spectroscopic data [10–12], NO is adsorbed on CoZSM-5 with the formation of mono- and dinitrosyl complexes of cobalt, whereas nitrite–nitrate complexes are additionally formed in the presence of oxygen. Moreover, the formation of adsorption complexes with an absorption band at about 2130 cm^{-1}, which were assigned to $NO_2^{\delta+}$ species additionally bound to the acidic OH groups of a zeolite, has been reported in a number of publications [10–12, 18–22]. Presently, the reactivity of [NO_x] species toward methane is still an open question. It is believed [10–12, 14] that these are nitrite or nitrate compounds. At the same time, data on the participation of $NO_2^{\delta+}$ species in the reduction of NO on CuZSM-5 [19] and HZSM-5 [20] catalysts were reported.

Previously, with the use of *in situ* diffuse-reflectance IR spectroscopy [17], we detected three types of adsorption complexes formed in the course of the simultaneous adsorption of NO and O_2 on a CoZSM-5 catalyst: cobalt mononitrosyls (a band at 1930 cm^{-1}), nitrite–nitrate complexes (1523 cm^{-1}), and $NO_2^{\delta+}$ species (2130 cm^{-1}). On the addition of methane to a mixture of NO and O_2, the concentration of nitrite–nitrate and $NO_2^{\delta+}$ species considerably decreased; this fact was indicative of the active participation of these species in the reaction. Based on an analysis of isotope transfer processes with the replacement of $^{14}N^{16}O$ by $^{15}N^{18}O$ in a mixture of NO + O_2 [23], as well as NO + O_2 + CH_4 [24], the rates of formation of adsorbed [NO_x] complexes as functions of oxygen concentration in mixtures and the rates of their conversion into N_2 were determined. As a result, it was demonstrated that molecular nitrogen is formed with the participation of both $NO_2^{\delta+}$ species and nitrite–nitrate complexes. In the former case, the rate of the reaction was higher than that in the latter case by a factor of ~2.5. Nevertheless, some aspects that are crucial for understanding the mechanism of this reaction remained questionable. In particular, the conversion of carbon-containing intermediates on the catalyst surface in CO_2, as well as the participation of these species in the transformations of nitrogen-containing intermediates in N_2, in accordance with a mechanism proposed based on the isotope studies of ^{15}N-label transfer, remained unclear.

Therefore, in this work, we studied the dynamics of carbon-label transfer on the replacement of $^{12}CH_4$ with $^{13}CH_4$ under conditions of the steady-state reaction of NO reduction with methane. The experiments were performed under conditions similar to those in experiments with labeled nitrogen oxide. Based on the numerical simulation of isotopic response curves, the reaction scheme of methane conversion into CO_2 was determined, and the concentrations and reaction rates of intermediates were estimated as functions of reactant concentrations and temperature. As a result, we revealed differences in the kinetics of the reaction via

0023-1584/04/4503-0436 © 2004 MAIK "Nauka/Interperiodica"

pathways with the participation of $NO_2^{\delta+}$ species and nitrite–nitrate complexes and, after a comparison with isotope data on $^{15}N^{18}O$, gained a clearer insight into the reaction mechanism.

EXPERIMENTAL

The CoZSM-5 catalyst used in our experiments was synthesized in accordance with the procedure described elsewhere [14]. Note that it was prepared by the ion exchange of HZSM-5 zeolite (with a SiO_2/Al_2O_3 ratio equal to 37) with a $Co(NO_3)_2$ solution followed by drying and calcination at 500°C. The cobalt content of the catalyst was 1.8 wt %, which corresponds to 2×10^{20} (atom Co)/(g Cat). X-ray diffraction data showed that the catalyst was free of a cobalt oxide phase. According to EXAFS data, cobalt occurred as small oxide-like clusters with a tetrahedral oxygen environment [14].

The SSITKA experiments were performed as described below. Before an experiment, the catalyst was held in a mixture of $6\%O_2$ + He at 500°C for 1 h and then cooled in the same flow to a temperature at which the experiment was performed. Next, a reaction mixture of $NO + CH_4 + O_2 + He$ was introduced into the reactor; after the attainment of steady-state reaction conditions (usually, in 8–10 min), the reaction mixture was stepwise replaced with a mixture of the same chemical composition containing, however, carbon-labeled methane $^{13}CH_4$ (98% enrichment). As an isotopic equilibrium was approached, the dynamics of ^{13}C-label transfer from methane to CO_2 (CO was not found in the reaction products) were measured. The experiments were performed in a U-shaped quartz reactor placed in a gradientless furnace. The diffusion of a gas-flow front in this reactor was not greater than 1 s, as determined with the use of argon added to the reaction mixture in an amount of 0.1%. This allowed us to ignore diffusion effects in the numerical simulation of SSITKA data.

The chemical and isotopic composition of a gas mixture at the reactor outlet was detected with the use of a VG SENSORLAB 200D quadrupole mass spectrometer, which simultaneously recorded up to 16 masses. The quantitative analysis of mass-spectrometric data was performed with the use of spectra recorded for calibration gas mixtures with known concentrations of reaction mixture components. The concentrations of H_2O, NO, O_2, $^{12}CO_2$, and $^{13}CO_2$ were determined from the intensities of parent peaks with m/z = 18, 30, 32, 44, and 45, respectively. The concentrations of N_2 and $^{13}CH_4$ were determined from the intensities of peaks with m/z = 28 and 17, respectively, from which the known contributions of CO_2 and H_2O (CO^+ and OH^+ fragments) were subtracted beforehand. The concentration of $^{12}CH_4$ was determined from the intensity of a fragment with m/z = 15 after the subtraction of the known contribution of $^{13}CH_4$ from this intensity.

A catalyst fraction of 0.3–0.7 mm was used in all of the above experiments; the catalyst weight was 0.1 g, and the gas flow rate was 2 ml/s. Experiments on the isotopic substitution of $^{13}CH_4$ for $^{12}CH_4$ were performed under varying concentrations of CH_4, NO, and O_2 in the starting mixture and temperature. Nine experiments were performed in all at three different values of each of the parameters. Table 1 summarizes the initial concentrations and the conversions of CH_4 and NO. Based on the concentrations (C) of all isotopomers for each of the substances, the isotope fractions of ^{13}C in CH_4 and CO_2 were calculated as follows:

$$\alpha_{^{13}CH_4} = \frac{C(^{13}CH_4)}{C(^{13}CH_4) + C(^{12}CH_4)},$$

$$\alpha_{^{13}CO_2} = \frac{C(^{13}CO_2)}{C(^{13}CO_2) + C(^{12}CO_2)}.$$

EXPERIMENTAL RESULTS

Figures 1a–4a demonstrate changes in the isotope fraction of ^{13}C in CH_4 and CO_2 molecules with time at the reactor outlet after the replacement of a starting mixture of $^{12}CH_4 + NO + O_2 + He$ by a mixture of $^{13}CH_4 + NO + O_2 + Ar + He$. It can be seen that the fraction of ^{13}C in CH_4 increased almost synchronously with the argon concentration. In this case, the shapes of the curves depended only slightly on the reaction conditions. A small shift (on the order of 1 s) of the function $\alpha_{^{13}CH_4}(t)$ with respect to the response curve of argon was commensurable with the time resolution of the mass spectrometer, and it was most likely due to the weak absorption of methane in zeolite channels.

As distinct from methane, the concentration of the ^{13}C label in CO_2 increased more slowly in all of the experiments, and the function $\alpha_{^{13}CO_2}(t)$ was noticeably shifted with respect to the response curves of argon and methane. As was found previously [25, 26], the qualitative features of the reaction mechanism can be determined from the shape of isotopic response curves plotted as the logarithmic dependence of the isotope fraction on time. This dependence is strictly linear if the reaction occurs by a consecutive mechanism. As can be seen in Figs. 1b–4b, in our case, the logarithmic function $\alpha_{^{13}CO_2}(t)$ is represented by a concave curve (convex downwards), which is characteristic of reactions that occur by a mechanism with parallel steps or by a consecutive mechanism with a buffer step. Based on the currently available notions of the mechanism of this reaction [17, 24], a parallel (two-pathway) mechanism

Table 1. Conditions of SSITKA experiments

Experiment no.	*T*, °C	Initial concentration, vol %			Conversion, %	
		NO	O_2	CH_4	NO	CH_4
1	450	0.3	3.0	**0.3**	31.4	15.6
2	450	0.3	3.0	0.4	39.9	15.7
3	450	0.3	3.0	**0.6**	48.5	12.8
4	450	0.3	**0.3**	0.4	32.3	12.5
5	450	0.3	**0.6**	0.4	27.1	11.2
6	450	**0.2**	3.0	0.4	53.1	19.1
7	450	**0.35**	3.0	0.4	39.0	17.7
8	**400**	0.3	3.0	0.4	44.9	6.2
9	**480**	0.3	3.0	0.4	66.8	44.9

of CO_2 formation due to the reactions of methane with various adsorbed NO species seems most probable.

The shape of the isotopic response curves of $\alpha_{^{13}CO_2}(t)$ remained unchanged on varying the temperature and composition of a starting mixture; however, the rate of isotopic substitution in CO_2 changed noticeably (Figs. 1–4). Changes in the concentrations of methane and NO had almost no effect on the isotopic response dynamics (Figs. 1, 2), whereas the rate of ^{13}C transfer to CO_2 noticeably increased as the concentration of oxygen and the temperature were increased (Figs. 3, 4). It is well known that the rate of isotopic substitution is determined by the ratio of the rate of reaction (r) to the concentration of intermediate compounds (θ). Consequently, the ratio r/θ remained unchanged on varying the concentrations of methane and NO, whereas it increased with oxygen concentration and temperature. This means that the rate of conversion of surface intermediates, which are formed by the interaction of methane with $[NO_x]$, is practically independent of the concentration of NO; however, it essentially depends on oxygen concentration and temperature. Next, based on a numerical simulation of the dynamics of ^{13}C-label transfer, we attempted to determine the rates of reaction via either of the pathways and

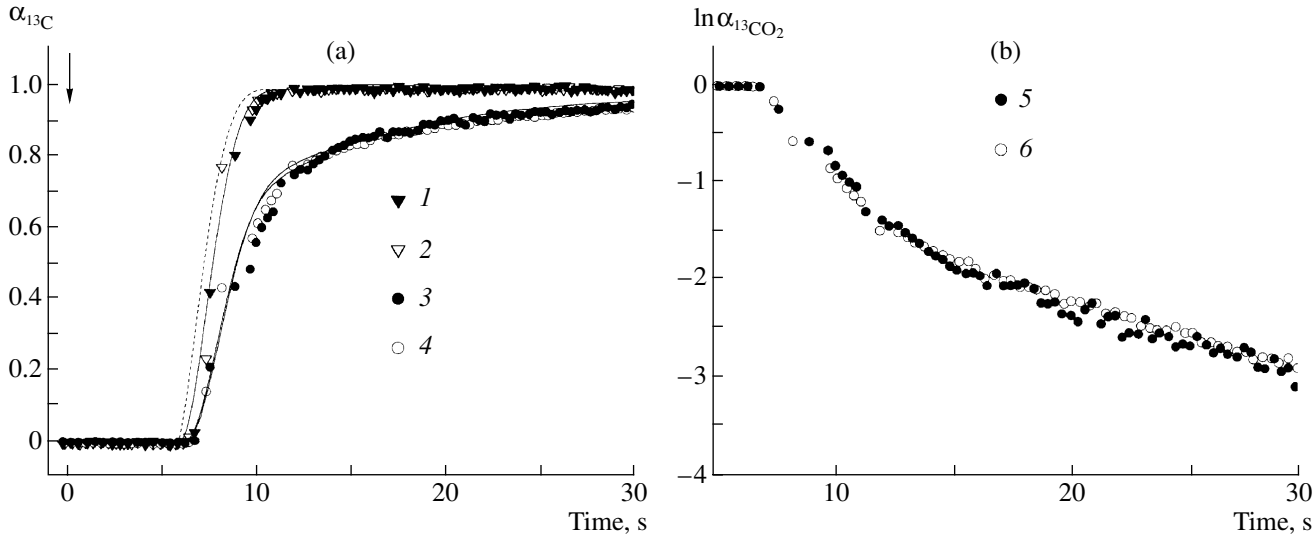

Fig. 1. Changes in (a) the isotope fraction of ^{13}C in (*1*, *2*) CH_4 and (*3*, *4*) CO_2 and (b) the logarithm of the isotope fraction of ^{13}C in (*5*, *6*) CO_2 with time at (*1*, *3*, *5*) $C_{CH_4} = 0.3\%$ and (*2*, *4*, *6*) $C_{CH_4} = 0.6\%$ (experiment nos. 1 and 3 in Table 1, respectively). Points, solid lines, and the dashed line indicate experimental data, calculated data, and argon, respectively. The arrow indicates the point in time at with an isotope mixture was introduced.

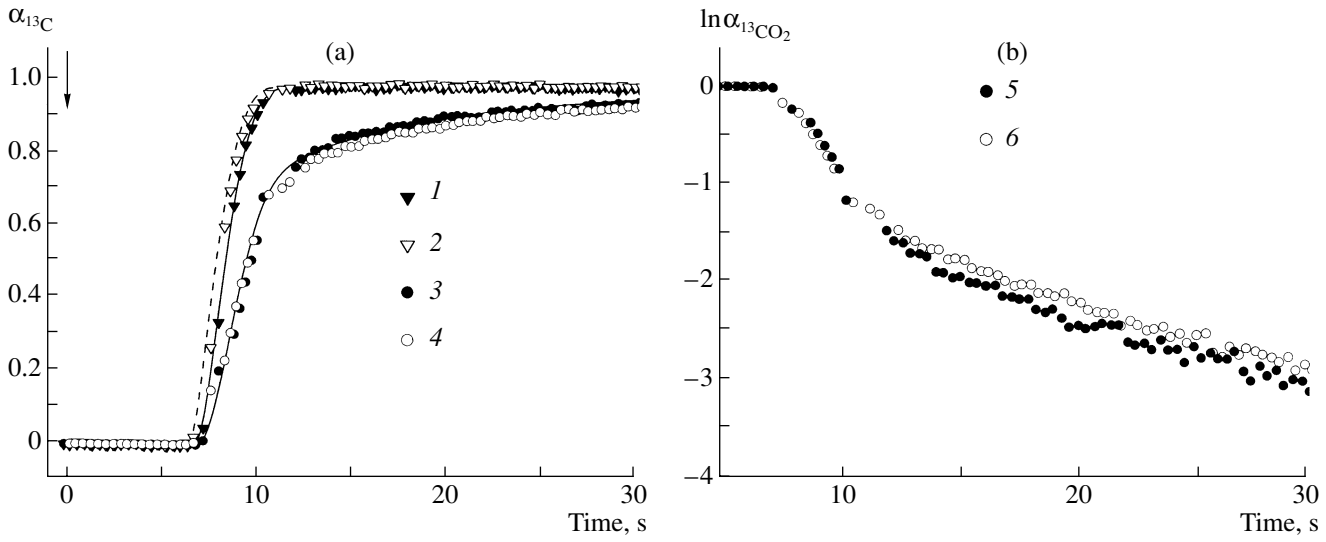

Fig. 2. Changes in (a) the isotope fraction of ^{13}C in (*1*, *2*) CH_4 and (*3*, *4*) CO_2 and (b) the logarithm of the isotope fraction of ^{13}C in (*5*, *6*) CO_2 with time at (*2*, *4*, *6*) $C_{NO} = 0.2$ and (*1*, *3*, *5*) 0.35% (experiment nos. 6 and 7 in Table 1, respectively). Points, solid lines, and the dashed line indicate experimental data, calculated data, and argon, respectively. The arrow indicates the point in time at with an isotope mixture was introduced.

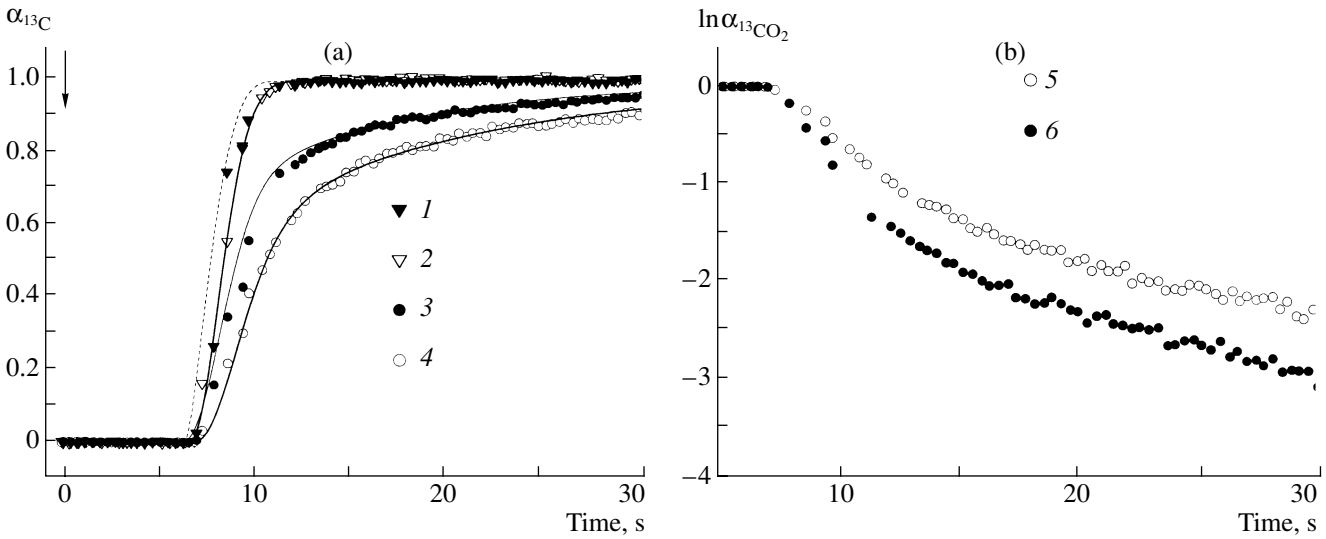

Fig. 3. Changes in (a) the isotope fraction of ^{13}C in (*1*, *2*) CH_4 and (*3*, *4*) CO_2 and (b) the logarithm of the isotope fraction of ^{13}C in (*5*, *6*) CO_2 with time at (*1*, *3*, *5*) $C_{O_2} = 3.0$ and (*2*, *4*, *6*) 0.3% (experiment nos. 2 and 4 in Table 1, respectively). Points, solid lines, and the dashed line indicate experimental data, calculated data, and argon, respectively. The arrow indicates the point in time at with an isotope mixture was introduced.

to evaluate the concentrations of key intermediates and the rate constants of the steps of their conversion.

NUMERICAL SIMULATION RESULTS

A dynamic model for isotope transfer in a steady-state reaction in a plug-flow reactor is represented as a set of hyperbolic differential equations, which reflect changes in the concentration of a label isotope in the reaction components with time and along the reactor length [26, 27]. The form of the right-hand sides of the equations depends on the mechanism of the reaction. Initially, it was assumed that the reaction can occur via several parallel pathways and the steps of methane interaction with $[NO_x]$ and all the subsequent reactions of C,N-containing surface compounds to form CO_2 are irreversible. Then, the reaction scheme of methane conversion into CO_2 can be represented as follows:

$$\mathrm{CH_4} \rightarrow \begin{cases} [Z_1\text{–C...N}]_1 \rightarrow \ldots \rightarrow [Z_1\text{–C...N}]_j \rightarrow \ldots \rightarrow \mathrm{CO_2} & r_1 \\ [Z_i\text{–C...N}]_1 \rightarrow \ldots \rightarrow [Z_i\text{–C...N}]_j \rightarrow \ldots \rightarrow \mathrm{CO_2} & r_i \\ [Z_n\text{–C...N}]_1 \rightarrow \ldots \rightarrow [Z_n\text{–C...N}]_j \rightarrow \ldots \rightarrow \mathrm{CO_2} & r_n, \end{cases}$$

where $[Z_i\text{–C...N}]_j$ refers to intermediate C,N-containing compounds.

A model of ^{13}C-label transfer from CH_4 to CO_2 corresponding to the above scheme has the form

$$\frac{\partial C_{\mathrm{CH_4}}\alpha_{\mathrm{CH_4}}}{\partial t} + \frac{U}{V}\frac{\partial C_{\mathrm{CH_4}}\alpha_{\mathrm{CH_4}}}{\partial \xi} = -\frac{G}{VN}\sum_{i=1}^{n} r_i\alpha_{\mathrm{CH_4}},$$

$$\theta_{i1}\frac{\partial \alpha_{ij}}{\partial t} = r_i\alpha_{\mathrm{CH_4}} - r_i\alpha_{i1},$$

$$\ldots\ldots\ldots\ldots\ldots\ldots\ldots \qquad (1)$$

$$\theta_{ij}\frac{\partial \alpha_{ij}}{\partial t} = r_i\alpha_{ij-1} - r_i\alpha_{ij},$$

$$\frac{\partial C_{\mathrm{CO_2}}\alpha_{\mathrm{CO_2}}}{\partial t} + \frac{U}{V}\frac{\partial C_{\mathrm{CO_2}}\alpha_{\mathrm{CO_2}}}{\partial \xi} = \frac{G}{VN_\mathrm{A}}\sum_{i=1}^{n} r_i\alpha_{im}.$$

The initial and boundary conditions are as follows:

$$t = 0: \quad \alpha_{ij} = 0,\ \alpha_{\mathrm{CO_2}} = 0,\ \alpha_{\mathrm{CH_4}} = 0,$$

$$\xi = 0: \quad \alpha_{\mathrm{CH_4}} = 0.98,$$

where $C_{\mathrm{CH_4}}$ and $C_{\mathrm{CO_2}}$ are the concentrations of CH_4 and CO_2 in a gas phase, vol %; θ_{ij} is the surface concentration of a C,N-containing compound formed via the *i*th pathway at the *j*th step, molecule/g; α_{ij} is the isotope fraction of the ^{13}C label as a constituent of θ_{ij}; r_i is the rate of the reaction via the *i*th pathway, molecule g^{-1} s^{-1}; *n* is the number of reaction pathways; *m* is the number of reaction steps in every pathway; *V* is the reactor volume, cm^3; *U* is the gas flow rate, cm^3/s; *G* is the catalyst sample weight, g; N_A is Avogadro number; *t* is time, s; and ξ is the dimensionless length of the catalyst bed.

The number of reaction pathways (*n*), the rates of reaction via these pathways (r_i), and the concentrations of C,N-containing compounds θ_{ij} were determined by numerical analysis of the set of Eqs. (1) so that the experimental curves of $\alpha(t)$ were identical with the calculated curves. As a result, we found that the conversion of methane into CO_2 occurs via two main pathways and evaluated the rates of reaction via these pathways. Note that the results of the simulation do not exclude the occurrence of other pathways; however, the contribution of these pathways to the overall rate of CO_2 formation is negligibly small. Unfortunately, SSITKA did not allow us to detail the reaction sequences of C,N-containing intermediates because of the inadequate time resolution of the procedure. Therefore, we evaluated only the total concentrations of C,N-containing compounds formed in each of the main pathways. Table 2 summarizes the rates of reaction via the two designated pathways and the concentrations of C,N-containing intermediates. The calculated functions

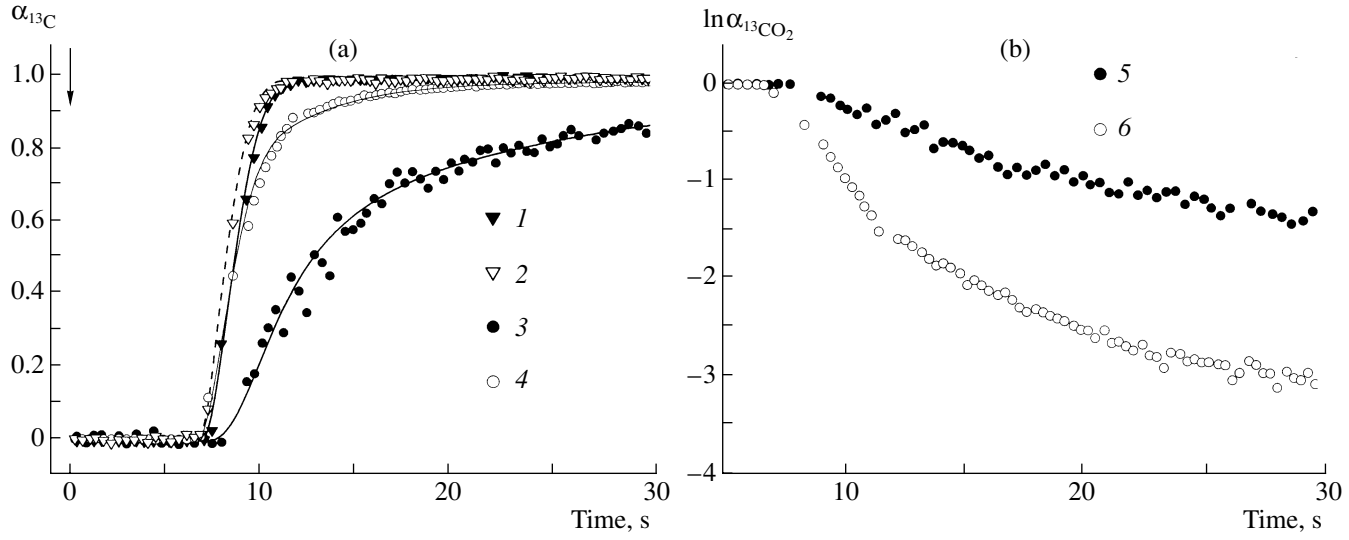

Fig. 4. Changes in (a) the isotope fraction of ^{13}C in (*1*, *2*) CH_4 and (*3*, *4*) CO_2 and (b) the logarithm of the isotope fraction of ^{13}C in (*5*, *6*) CO_2 with time at (*1*, *3*, *5*) $T = 400$ and (*2*, *4*, *6*) 480°C (experiment nos. 8 and 9 in Table 1, respectively). Points, solid lines, and the dashed line indicate experimental data, calculated data, and argon, respectively. The arrow indicates the point in time at with an isotope mixture was introduced.

Table 2. Calculated values of the rates of CO_2 formation via different pathways and the concentrations of surface [Z_i–C...N] complexes

T, °C	Initial concentration, vol %			Rate of CO_2 formation $\times 10^{-18}$, molecule g^{-1} s^{-1}			Concentration $\times 10^{-18}$, molecule/g	
	NO	O_2	CH_4	r_1	r_2	r_1/r_2	[Z_1–C...N]	[Z_2–C...N]
450	0.3	3.0	**0.3**	0.19	0.08	2.4	0.16	0.8
	0.3	3.0	**0.4**	0.25	0.11	2.3	0.22	1.0
	0.3	3.0	**0.6**	0.30	0.14	2.2	0.26	1.5
450	0.3	**0.3**	0.4	0.18	0.10	1.8	0.28	1.4
	0.3	**0.6**	0.4	0.16	0.10	1.6	0.20	1.3
	0.3	**3.0**	0.4	0.25	0.11	2.3	0.22	1.0
450	**0.2**	3.0	0.4	0.30	0.14	2.1	0.22	1.4
	0.3	3.0	0.4	0.25	0.11	2.3	0.22	1.0
	0.35	3.0	0.4	0.28	0.12	2.3	0.20	1.1
400	0.3	3.0	0.4	0.08	0.04	2.0	0.20	1.0
450	0.3	3.0	0.4	0.25	0.11	2.3	0.22	1.0
480	0.3	3.0	0.4	0.74	0.28	2.6	0.06	1.1

$\alpha_{^{13}CO_2}(t)$ obtained based on the two-pathway reaction scheme are practically identical to the experimental functions (Figs. 1–4); differences between them lie within the limits of experimental error.

DISCUSSION

An analysis of the dynamics of carbon-label transfer demonstrated that the formation of CO_2 in the reduction of nitrogen oxide with methane occurs via two parallel pathways. The rate of methane conversion into CO_2 via the first pathway is several times higher than that via the second pathway. At 450°C in an excess of oxygen (C_{O_2} = 3.0%), the ratio between the rates of CO_2 formation via these pathways is approximately constant; it is practically independent of the NO and methane concentrations in the mixture and equals ~2.3. This is consistent with the ratio between the rates of reactions that occur via $NO_2^{\delta+}$ species and nitrite–nitrate complexes, which were evaluated previously from isotope experiments with $^{15}N^{18}O$ [24]. On this basis, we assume that the formation of CO_2 via the first (rapid) pathway results from the interaction of methane with $NO_2^{\delta+}$ species, whereas CO_2 is formed as a result of the interaction of methane with surface nitrite–nitrate complexes in the second case.

It is well known that the formation of nitrite–nitrate complexes is associated with the presence of transition metal cations or transition metal oxide clusters in zeolite channels [4, 9–17]. As for $NO_2^{\delta+}$, the formation of these species has been observed on a number of catalysts (NaZSM-5, CoZSM-5, and FeZSM-5) including HZSM-5 [11, 12, 17–22]. Therefore, it is believed that they are associated with the strong proton sites of zeolites, and they can be stabilized in the presence of transition metal cations [12, 17, 19, 20]. This also follows from data obtained previously using *in situ* diffuse-reflectance IR spectroscopy on the same catalyst sample that exhibited a clear correlation between the rate of formation of $NO_2^{\delta+}$ species and a decrease in the band intensities of zeolite hydroxyl groups [17]. Moreover, the results of experiments with labeled $^{15}N^{18}O$ suggest that the oxygen exchange of CoO_x clusters with the mononitrosyl complexes of cobalt and nitrite–nitrate complexes occurs much more rapidly than with $NO_2^{\delta+}$ species. Thus, it is reasonable to consider that nitrite–nitrate complexes and $NO_2^{\delta+}$ species are related to different sites: the former are related to Co^{2+} ions (or CoO_x clusters), whereas the latter are related to the

paired sites $Co^{2+}\cdots OH$ localized at the interface between CoO_x clusters and the zeolite lattice, which, probably, contains strong proton sites. Therefore, we believe that the former (faster) reaction pathway occurs on $Co^{2+}\cdots OH$ sites, whereas the latter (slower) occurs on Co^{2+} sites:

$$CH_4 \xrightarrow{+[NO_2^{\delta+}]} [Z_1\text{–}C\ldots N] \longrightarrow CO_2\ (+ N_2 + H_2O) \quad \text{fast}$$
$$CH_4 \xrightarrow{+[ONO_x]} [Z_2\text{–}C\ldots N] \longrightarrow CO_2\ (+ N_2 + H_2O) \quad \text{slow},$$

where $[ONO_x]$ refers to nitrite–nitrate complexes, and $[Z_1\text{–}C\ldots N]$ and $[Z_2\text{–}C\ldots N]$ refer to intermediates localized on $Co^{2+}\cdots OH$ and Co^{2+} sites, respectively.

As mentioned above, a change in the concentration of methane and NO has practically no effect on the ratio between the rates of reaction via different pathways. At the same time, Table 2 indicates a clear trend toward decreasing the contribution of the former pathway to the overall reaction rate as the concentration of oxygen in the mixture was decreased. In other words, the dependence of the rate of the reaction on $Co^{2+}\cdots OH$ sites on the concentration of oxygen was stronger than that on Co^{2+} sites. A change in the temperature also more strongly affected the rate of reaction on $Co^{2+}\cdots OH$ sites. Differences in the kinetics of the reaction via the identified pathways became more clearly pronounced on going to relative rates normalized to the number of active sites, that is, the turnover numbers of the reaction.

Previously [23], we evaluated the number of paired $Co^{2+}\cdots OH$ sites in special isotope experiments with labeled $^{15}N^{18}O$, in which the concentrations of NO and O_2 were varied over a wide range. We found that, starting with concentrations of NO and O_2 equal to 0.6 and 1.5%, respectively, the concentration of $NO_2^{\delta+}$ species ceased to increase. Assuming that in this case the limiting coverage of sites is reached, we can estimate the number of $Co^{2+}\cdots OH$ sites, which was approximately 10% of the total number of cobalt atoms in the catalyst.

Thus, taking the number of Co^{2+} sites equal to the total number of cobalt atoms (2×10^{20} molecule/g) and the number of $Co^{2+}\cdots OH$ sites equal to 2×10^{19} molecule/g, we calculated the rates of reaction via either of the pathways referenced to the number of sites and the coverages with $[Z_1\text{–}C\ldots N]$ and $[Z_2\text{–}C\ldots N]$ intermediates (Table 3). It can be seen that the turnover number of the reaction on $Co^{2+}\cdots OH$ sites is greater than that on Co^{2+} sites by a factor of ~20–25, whereas the coverage

Table 3. Turnover numbers of the reaction via different pathways, surface coverages with $[Z_i\text{–}C...N]$ complexes, and apparent rate constants of their conversion

T, °C	Initial concentration, vol %			Turnover number × 10^2, s^{-1}		Surface coverage, %		k^{app}, s^{-1}	
	NO	O_2	CH_4	pathway 1	pathway 2	$[Z_1\text{–}C...N]$	$[Z_2\text{–}C...N]$	$[Z_1\text{–}C...N]$	$[Z_2\text{–}C...N]$
450	0.3	3.0	**0.3**	0.95	0.04	0.8	0.4	1.18	0.10
	0.3	3.0	**0.4**	1.25	0.055	1.1	0.5	1.14	0.11
	0.3	3.0	**0.6**	1.50	0.07	1.3	0.75	1.15	0.09
450	0.3	**0.3**	0.4	0.90	0.05	1.4	0.7	0.64	0.07
	0.3	**0.6**	0.4	0.80	0.05	1.0	0.65	0.80	0.08
	0.3	**3.0**	0.4	1.25	0.055	1.1	0.5	1.14	0.11
450	**0.2**	3.0	0.4	1.50	0.07	1.1	0.7	1.36	0.10
	0.3	3.0	0.4	1.25	0.055	1.1	0.5	1.14	0.11
	0.35	3.0	0.4	1.40	0.06	1.0	0.55	1.40	0.11
400	0.3	3.0	0.4	0.40	0.02	1.0	0.5	0.40	0.04
450	0.3	3.0	0.4	1.25	0.055	1.1	0.5	1.14	0.11
480	0.3	3.0	0.4	3.70	0.14	0.3	0.55	12.30	0.25

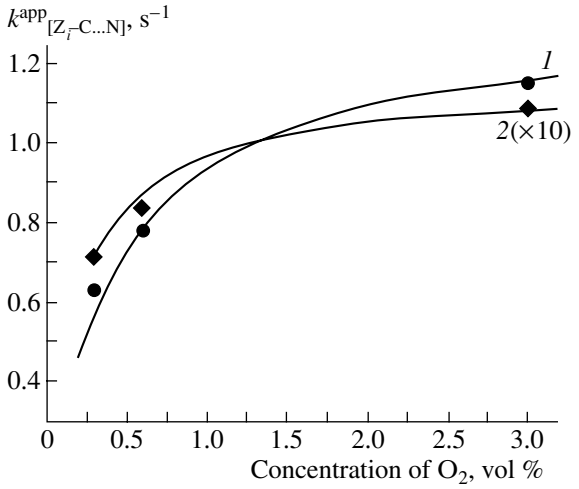

Fig. 5. Dependence of the apparent rate constant of the conversion of $[Z_i–C\cdots N]$ intermediates formed via (*1*) the first and (*2*) the second pathways on the concentration of oxygen. Points and curves refer to experimental results and data calculated from Eq. (3).

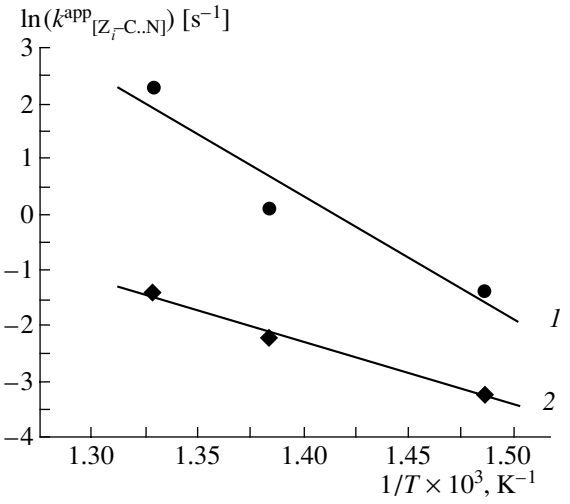

Fig. 6. Arrhenius plots for the rate constants of conversion of $[Z_i–C\ldots N]$ intermediates formed via (*1*) the first and (*2*) the second pathways of the reaction of selective nitrogen oxide reduction with methane.

of active sites with $[Z_1–C\ldots N]$ and $[Z_2–C\ldots N]$ intermediates is about 1% or lower. These low coverages suggest that the rate constants of the steps of $[Z_1–C\ldots N]$ and $[Z_2–C\ldots N]$ transformations are comparatively high, and the steps of formation of $[NO_x]$ complexes and/or the steps of $[NO_x]$ interaction with methane are the rate-limiting steps of the reaction via both of the pathways. As can be seen in Tables 2 and 3, among all of the initial reactants (NO, O_2, and CH_4), the concentration of methane has the greatest effect on the rate of the reaction. Indeed, a twofold increase in the concentration of CH_4 increased the rate of the reaction by a factor of 1.5–1.8, whereas approximately the same change in the concentration of NO had practically no effect on the rate of the reaction. As the concentration of oxygen was increased by one order of magnitude, the rates of the reaction increased by only 10–20%. This allowed us to assume that the rate of the reaction via either the former or the latter pathway is limited by the steps of methane interaction with $NO_2^{\delta+}$ species and nitrite–nitrate complexes. It is most likely that the relatively weak dependence of the rate of the reaction on the concentration of NO and O_2 is due to the reversibility of the steps of formation of NO_x complexes.

Although the steps of conversion of $[Z_i–C\ldots N]$ intermediates into CO_2 are fast, a study of the kinetics of these steps is important because it will provide an opportunity to gain deeper insight into the reaction mechanism. The ratio of the turnover number to the coverage with $[Z_i–C\ldots N]$ intermediates is nothing else than the apparent rate constant of conversion of these intermediates. The data in Table 3 indicate that the apparent rate constants of $[Z_i–C\ldots N]$ conversion on $Co^{2+}\cdots OH$ are higher than those on Co^{2+} by more than one order of magnitude. Moreover, note that the dependence of the rate constants of conversion of $[Z_i–C\ldots N]$ intermediates upon the concentration of oxygen on $Co^{2+}\cdots OH$ sites is stronger than that on Co^{2+} sites (Fig. 5). Based on these relationships, we can evaluate the rate constant of the interaction of $[Z_i–C\ldots N]$ intermediates with oxygen. Representing the conversion of $[Z_i–C\ldots N]$ into CO_2 as a sequence of elementary steps at one of which the reaction with oxygen occurs and expressing the rate of this step as $r_i = k_i^{ox}\theta_{[Z_i–C\ldots N]_j} C_{O_2}$ and the rates of all the other steps as $r_i = k_i^j\theta_{[Z_i–C\ldots N]_j}$ (where k_i^j is the rate constant of the jth step via the ith pathway), the rate of the reaction via either of the pathways can be expressed as follows:

$$r_i = \frac{\sum\theta_{[Z_i–C\ldots N]_j}}{\dfrac{1}{k_i^{ox}C_{O_2}} + \sum\dfrac{1}{k_i^j}}, \qquad (2)$$

where $\sum\theta_{[Z_i–C\ldots N]_j}$ s the sum of the concentrations of all the C,N-containing intermediates formed via a given pathway, that is, the value of $\theta_{[Z_i–C\ldots N]}$, which is determined from experimental data. Equation (2) can be put in the form

$$k^{app}_{[Z_i–C\ldots N]} = \frac{r_i}{\sum\theta_{[Z_i–C\ldots N]_j}} = 1\Big/\left(\frac{1}{k_i^{ox}C_{O_2}} + \sum\frac{1}{k_i^j}\right). \qquad (3)$$

Thus, we expressed the apparent rate constants of the conversion of $[Z_i–C\ldots N]$ intermediates in terms of the rate constants of elementary steps and the concentra-

tion of oxygen. Equation (3) adequately describes the experimental dependence of the rate constants of the conversion of [Z_i–C…N] intermediate compounds on the concentration of oxygen (Fig. 5).

The found rate constants of the steps of interaction with oxygen via the first and second pathways are k_1^{ox} = 380 s^{-1} and k_2^{ox} = 50 s^{-1}, respectively.

The higher value of the rate constant k_1^{ox}, as compared with k_2^{ox}, could be due to the features of molecular oxygen adsorption. Previously [23], we found that the mechanism of formation of $NO_2^{\delta+}$ species includes a step of dissociative oxygen adsorption. It is most likely that this adsorption occurs at the interface between cobalt oxide clusters and zeolite. We concluded that oxygen did not undergo dissociative adsorption on the clusters themselves. This conclusion was based on the fact that an oxygen label, which rapidly entered into the composition of CoO_x clusters, did not appear in the gas-phase oxygen in the course of the isotopic substitution of $^{15}N^{18}O$ for $^{14}N^{16}O$. It is reasonable to assume that the dissociatively adsorbed oxygen species that reacts with NO to form $NO_2^{\delta+}$ can participate in the oxidation of [Z_i–C…N] intermediate compounds. In this case, the probability of this interaction with [Z_1–C…N] intermediates, which are also localized at the interface between oxide clusters and zeolite, is higher than that with [Z_2–C…N]. The Arrhenius plots of the rate constants of conversions of [Z_1–C…N] and [Z_2–C…N] intermediates (Fig. 6) can also be interpreted in terms of these concepts. It can be seen that the apparent activation energy via the first reaction pathway (44 kcal/mol) is twice as high as that via the second pathway (22 kcal/mol). The former of the estimated values can correspond to the activation energy of the step of dissociative oxygen adsorption, and the latter can correspond, for example, to the activation energy of the diffusion of adsorbed oxygen to active sites, where nitrite–nitrate complexes are formed. Note that the above considerations are preliminary, and the possibility of dissociative oxygen adsorption on the oxide-like cobalt clusters cannot be completely excluded, although the rates are lower than that on interfacial sites. Additional detailed studies with the use of labeled molecular oxygen should be performed in order to clarify this question.

Thus, the study of the dynamics of ^{13}C-label transfer demonstrated that the reaction of NO reduction with methane on CoZSM-5 in the presence of molecular oxygen occurs via two parallel pathways: on Co^{2+} sites (or CoO_x clusters) and on paired $Co^{2+}\cdots OH$ sites localized at the interface of oxide-like cobalt clusters and zeolite. The interaction of methane with $NO_2^{\delta+}$ species (first pathway) or surface nitrite–nitrate complexes (second pathway) is the rate-limiting step of the reaction via either of the two pathways. The rate of the reaction on $Co^{2+}\cdots OH$ sites is higher than that on Co^{2+} by more than one order of magnitude. The main factors responsible for the rapid occurrence of the reaction on $Co^{2+}\cdots OH$ sites are, first, the presence of strong acid sites (which stabilize $NO_2^{\delta+}$ species, which are more reactive toward methane) at the interface with oxide-like cobalt clusters and, second, dissociative oxygen adsorption, which occurs at interfacial sites. The latter circumstance is favorable for the more rapid conversion of C,N-containing intermediates, which are formed in the reaction of $NO_2^{\delta+}$ with methane, into reaction products.

ACKNOWLEDGMENTS

This work was performed within the framework of a joint research program between the Boreskov Institute of Catalysis, Siberian Division, Russian Academy of Sciences and the Institut de Recherches sur la Catalyse (Lyon, France) and supported by the Russian Foundation for Basic Research (grant no. 00-03-22004).

REFERENCES

1. Vassallo, J., Miro, E., and Petunchi, J., *Appl. Catal., B*, 1995, vol. 7, p. 65.
2. Burch, R. and Scire, S., *Appl. Catal., B*, 1994, vol. 3, p. 295.
3. Li, Y. and Armor, J.N., *Appl. Catal., B*, 1993, vol. 2, p. 239.
4. Witzel, F., Sill, G.A., and Hall, W.K., *J. Catal.*, 1994, vol. 149, p. 229.
5. Petunchi, J.O. and Hall, W.K., *Appl. Catal., B*, 1993, vol. 2, p. 17.
6. Shelef, M., Montreuil, C.N., and Jen, H.W., *Catal. Lett.*, 1994, vol. 26, p. 277.
7. Konin, G.A., Il'ichev, A.N., Matyshak, V.A., Khomenko, T.I., Korchak, V.N., Sadykov, V.A., Doronin, V.P., Bunina, R.V., Alikina, G.M., Kuznetsova, T.G., Paukshtis, E.A., Fenelonov, V.B., Zaikovskii, V.I., Ivanova, A.S., Beloshapkin, S.A., Rozovskii, A.Y., Tretyakov, V.F., Ross, J.R.H., and Breen, J.P., *Top. Catal.*, 2001, vol. 16, p. 193.
8. Tretyakov, V.F., Burdeynaya, T.N., Davydova, M.N., Matyshak, V.A., and Glebov, L.S., *Top. Catal.*, 2001, vol. 16, p. 243.
9. Cowan, A.D., Dumpelmann, R., and Cant, N.W., *J. Catal.*, 1995, vol. 151, p. 356.
10. Li, Y., Slager, T.L., and Armor, J.N., *J. Catal.*, 1994, vol. 150, p. 388.
11. Bell, A.T., *Catal. Today*, 1997, vol. 38, p. 151.
12. Aylor, A.W., Lobree, L.J., Reimer, J.A., and Bell, A.T., *Stud. Surf. Sci. Catal.*, 1996, vol. 101, p. 661.
13. Adelman, B.J., Beutel, T., Lei, G.-D., and Sachtler, W.M.H., *J. Catal.*, 1996, vol. 158, p. 327.

14. Sadykov, V.A., Beloshapkin, S.A., Paukshtis, E.A., Alikina, G.M., Kochubei, D.I., Degtyarev, S.P., Bulgakov, N.N., Veniaminov, S.A., Netyaga, E.V., Bunina, E.V., Kharlanov, A.N., Lunina, E.V., Lunin, V.V., Matyshak, V.A., and Rozovskii, A.Ya., *Pol. J. Environ. Stud.*, 1997, vol. 6, p. 21.

15. Cowan, A.D., Cant, N.W., Haynes, B.S., and Nelson, P.F., *J. Catal.*, 1998, vol. 176, p. 329.

16. Lombardo, E.A., Sill, G.A., D'Itri, J.L., and Hall, W.K., *J. Catal.*, 1998, vol. 173, p. 440.

17. Pinaeva, L.G., Sadovskaya, E.M., Suknev, A.P., Goncharov, V.B., Sadykov, V.A., Balzhinimaev, B.S., Decamp, T., and Mirodatos, C., *Chem. Eng. Sci.*, 1999, vol. 54, p. 4327.

18. Hoost, T.E., Laframboise, K.A., and Otto, K., *Catal. Lett.*, 1995, vol. 33, p. 105.

19. Valyon, J. and Hall, W.K., *J. Phys. Chem.*, 1993, vol. 97, p. 1204.

20. Hadjiivanov, K., Saussey, J., Freysz, J.L., and Lavalley, J.C., *Catal. Lett.*, 1998, vol. 52, p. 103.

21. Iwamoto, M., Hidenori, Y., Mizuno, N., Zhang, W.-X., Mine, Y., Furukawa, H., and Kagawa, S., *J. Phys. Chem.*, 1992, vol. 96, p. 9360.

22. Beutel, T., Adelman, B.J., and Sachtler, W.M.H., *Appl. Catal., B*, 1996, vol. 9, p. 1.

23. Sadovskaya, E.M., Suknev, A.P., Pinaeva, L.G., Goncharov, V.B., Bal'zhinimaev, B.S., Chupin, C., and Mirodatos, C., *J. Catal.*, 2001, vol. 201, p. 159.

24. Sadovskaya, E.M., Suknev, A.P., Goncharov, V.B., Sadykov, V.A., and Bal'zhinimaev, B.S., *Proc. 9th Int. Symp. on Heterogeneous Catalysis*, 2000, p. 49.

25. Shannon, S. and Goodvin, J., *Chem. Rev.*, 1995, vol. 95, no. 3, p. 679.

26. Sadovskaya, E.M., Bulushev, D.A., and Bal'zhinimaev, B.S., *Kinet. Katal.*, 1999, vol. 40, no. 1, p. 61.

27. Happel, J., *Isotopic Assessment of Heterogeneous Catalysis*, Orlando: Academic, 1986.